Relationship between Interchain Spacing of Amorphous Polymers and Blend Miscibility as Determined by Wide-Angle X-Ray Scattering

A. F. HALASA,* G. D. WATHEN, W. L. HSU, B. A. MATRANA, and J. M. MASSIE

The Goodyear Tire & Rubber Company, Akron, OH 44305-0001

SYNOPSIS

The average molecular interchain spacing ($\langle R \rangle$) in Angstroms for amorphous polymers was calculated from the strong maximum in the wide-angle X-ray scattering (WAXS) diffraction scan using established equations. The half-width (HW) of the maximum was used to qualitatively describe the distribution of $\langle R \rangle$. $\langle R \rangle$ and HW for immiscible blends corresponded to the weighted average of $\langle R \rangle$ and HW of the homopolymers in the blend. $\langle R \rangle$ for a miscible blend (natural rubber and high-vinyl PBd) was much larger than the weighted average of $\langle R \rangle$ of the component homopolymers, indicating that a new amorphous molecular structure had developed. The larger $\langle R \rangle$ for the miscible blend indicates that the molecular chains are spread further apart, resulting in an increase in free volume to accommodate the new packing order. The single T_g of this blend was lower than predicted by the Gordon–Taylor equation.

INTRODUCTION

When X-rays of a given wavelength impinge upon atoms in a polymer, they are scattered. This scatter is dependent upon the order within the polymer. A typical crystalline wide-angle X-ray scattering (WAXS) diffraction photo consists of sharp concentric rings, indicating that the chain molecules are stacked in a regular, high degree of order. A radial density distribution function, or diffractogram, for a crystalline polymer consists of sharp lines or peaks that indicate distinct interatomic distances between highly ordered planes. The WAXS diffraction photo for a semicrystalline polymer consists of concentric rings superimposed on a halo, indicating an intermediate order, or less perfect crystal. The diffractogram for a semi-crystalline polymer has the X-ray scattering intensity spread, resulting in a diffractogram with wider peaks on a raised background that shows the interatomic distance of the less ordered crystalline planes and the amorphous scatter.

The WAXS diffraction photo for an amorphous polymer has a diffuse halo (or halos) indicating disorder. The diffractogram for an amorphous polymer, where the atoms are held together by a succession of chemical bonds, oscillates around a mean value and shows a distribution of average distance between the molecules. Although an amorphous polymer is disordered, the WAXS pattern will be governed by the configuration or special arrangement of bonds of fixed length and angles in the repeat unit of a given configuration in the polymer chain. Thus, molecular disorder in amorphous polymers can be measured by WAXS. The mean value or oscillating radial density distribution function (diffractogram) for an amorphous polymer will be unique due to the configuration and conformation of the polymer. This is illustrated in Figure 1 for three amorphous polybutadiene polymers with different vinyl contents. The position for the diffuse halo maximum and the diffraction band half-width are characteristic of the specific polybutadiene (Fig. 2 and Table II).

EXPERIMENTAL

A wide-angle X-ray equatorial scan of the unstretched, uncured polymer was made at room tem-

* To whom correspondence should be addressed.

Journal of Applied Polymer Science, Vol. 43, 183–190 (1991)
 CCC 0021-8995/91/010183-08$04.00

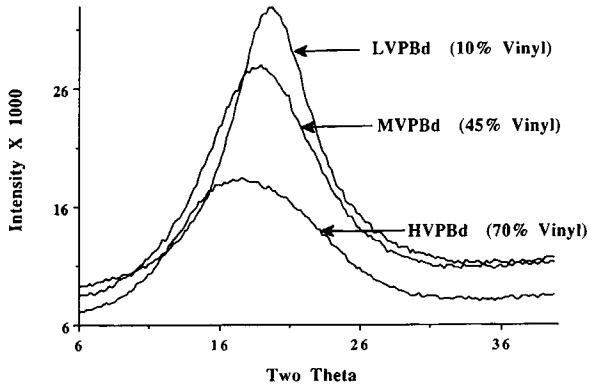

Figure 1 WAXS Diffractograms for Amorphous PBds.

Table I XRD Instrumentation

Rigaku Parameters
Cu targetpoint focus, Nickel filter
kV : 40, mA : 30
Pinhole collimator 1.0 mm d
Horizontal width limiting slit 2°
Vertical width limiting slit 2°
Rotating sample holder
Transmission mode
Sample perpendicular to X-ray beam
Step scan 6–40° (2 Θ)
Step width 0.200°
Counting time 10 sec

perature using a Rigaku DMax spectrometer. The flat specimen was 1 cm × 2 mm. X-ray diffraction measurements were taken by scanning the rotating sample from 6–40° (2 Θ) using the XRD parameters found in Table I. The intensity counts collected via the computer were corrected for polarization and absorption. No corrections were made for air scatter or incoherent scatter, which were considered negligible. The corrected intensity was smoothed and plotted vs. the (2 Θ) angle of diffraction. The position of the "peak maximum" was computed from the Bragg diffraction equation:

$$n\lambda = 2\,d \sin \Theta,$$

where n = order of reflection, λ = wavelength of radiation, d = interplanar distance, and 2 Θ = angle of diffraction.

The average interchain separation that gives rise to the strong maximum in the equatorial scan can be calculated from the following equation[1]:

$$\langle R \rangle = \tfrac{5}{8}(\lambda/\sin \Theta),$$

where $\langle R \rangle$ = average interchain separation in Angstroms, λ = the wavelength of radiation, and Θ = diffraction maximum angle.

The half-width (HW) of the WAXS amorphous maximum is the qualitative expression of the distribution of $\langle R \rangle$, and is calculated from the diffraction plot of 2 Θ vs. intensity. Using the Bragg equation, the d spacings are determined for the strong maximum at half-height intensity. The half-width is the difference between these two calculated d spacings.

An example of the calculation for $\langle R \rangle$ and HW for an amorphous PBd is shown in Figure 2.

Table II gives the experimental results for a variety of amorphous polymers. From repeated analyses of natural rubber samples at room temperature, the standard deviation for $\langle R \rangle$ was 0.02 Å and for HW 0.04 Å.

Table III gives the experimental results for the amorphous polymer blends examined.

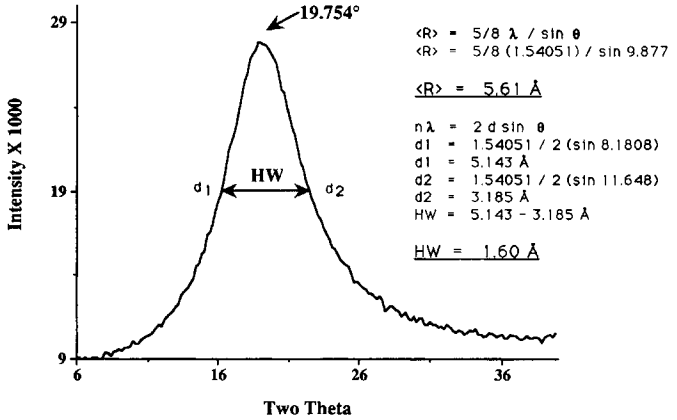

Figure 2 WAXS Diffractogram for Amorphous LVPBd (10% vinyl).

Table II Interchain Spacing for Amorphous Polymers

Polymer	Structure	2 Θ	⟨R⟩ (A°)	HW (A°)
Nickel cis-PBd	97% cis-1,4	19.000	5.84	1.62
Cobalt cis-PBd	98% cis-1,4	19.000	5.84	1.66
Neodymium cis-PBd	98.3% cis-1,4	19.151	5.79	1.63
Cobalt trans-PBd	80% trans-1,4	19.603	5.66	1.62
Linear HVPBd	70% vinyl	18.171	6.10	3.26
Linear MVPBd	45% vinyl	18.774	5.90	2.40
Linear LVPBD	10% vinyl	19.754	5.61	1.60
Branched MVPBd	45% vinyl	18.586	5.96	2.54
Natural rubber		18.472	6.00	2.18
Natural rubber		18.548	5.97	2.22
Natural rubber		18.548	5.97	2.24
Purified natural rubber		18.548	5.97	2.29
Natsyn 2200		18.472	6.00	2.35
E-SBR (50% styrene)	9% vinyl	19.452	5.70	2.05
E-SBR (23% styrene)	12% vinyl	19.452	5.70	1.91
E-SBR (18% styrene)	10% vinyl	19.565	5.67	1.72
S-SBR (23% styrene)	50% vinyl	18.849	5.88	2.76
S-SBR (18% styrene)	50% vinyl	18.586	5.96	2.84
S-SBR (25% styrene)	6% vinyl	19.490	5.69	1.69
S-SBR (25% styrene)	14% vinyl	19.452	5.70	1.60
S-SBR (25% styrene)	18% vinyl	19.377	5.72	2.17
Butyl rubber		14.177	7.80	2.16
Chlorobutyl rubber		14.365	7.70	2.16

HVPBd, high-vinyl polybutadiene; MVPBd, medium-vinyl polybutadiene; LVPBd, low-vinyl polybutadiene; Natsyn 2200, The Goodyear Tire & Rubber Co., synthetic natural rubber; E-SBR, emulsion styrene–butadiene copolymer; S-SBR, solution styrene–butadiene copolymer.

Table III Interchain Spacing for Amorphous Blends

Composition	2 Θ	⟨R⟩(Å)	HW(Å)
Immiscible blends			
50 NR/50 E-SBR (23% styrene)	19.000	5.83	2.12
50 NR/50 S-SBR (18% styrene)	19.075	5.81	2.05
50 NR/50 branched MVPBd	18.397	6.02	2.41
50 E-SBR (23% styrene)/50 Ni PBd	19.301	5.74	1.70
50 Ni-PBd/50 synthetic NR	18.887	5.96	1.93
50 LVPBD/50 Ni-PBd	19.565	5.67	1.65
50 LVPBD/50 synthetic NR	19.264	5.76	1.89
30 E-SBR/70 LVPBd	19.678	5.63	1.66
50 E-SBR/50 LVPBd	19.603	5.66	1.75
70 E-SBR/30 LVPBd	19.565	5.67	1.80
Miscible blends			
70 NR/30 HVPBd (70% vinyl)	18.359	6.04	2.47
50 NR/50 HVPBd (70% vinyl)	18.096	6.12	2.85
30 NR/70 HVPBD (70% vinyl)	18.055	6.14	3.06
50 NR/50 HVPBD (80% vinyl)	17.870	6.20	3.56

DISCUSSION

The interchain spacing for three structurally different amorphous polybutadienes [trans-PBd, cis-PBd made by different transition metal catalysts, and high-vinyl (70% 1, 2) PBd] was 5.66, 5.84, and 6.10 Å, while the *HW* was 1.62, 1.62, and 3.26 Å, respectively (Table III). The pendant vinyl group widens the molecular interchain distance and greatly increases the disorder between the PBd chains. A slightly smaller $\langle R \rangle$ is obtained for the PBd polymer of higher cis content (98.3%), compared to those with slightly lower cis-1,4 content. This suggests more efficient chain packing for high cis-1,4 PBd and is consistent with its reported higher low-temperature crystallinity.[2]

As seen in Table II, cis-PBd has an $\langle R \rangle$ of 5.84 Å, while cis-PI has an $\langle R \rangle$ of 5.97 Å. The methyl groups on the cis-PI (natural rubber) chain cause the chain separation to be larger than in cis-PBd. Butyl rubber has an $\langle R \rangle$ of 7.80 Å, and chlorobutyl rubber has an $\langle R \rangle$ of 7.70 Å. The bulky side groups in both butyl and chlorobutyl rubber cause steric hindrance, which greatly spreads the molecular chains apart.

The interchain spacing vs. % vinyl content for three linear PBd polymers, prepared with a lithium catalyst, are shown in Figure 3. The plot shows the influence of the vinyl group on the scattering pattern, and therefore on the chain spacing: $\langle R \rangle$ (70% vinyl) > $\langle R \rangle$ (45% vinyl) > $\langle R \rangle$ 10% vinyl. The *HW* or disorder also increases with vinyl content. Branched MVPBd with 45% vinyl content has an interchain spacing greater than linear MVPBd due to branched chains (Fig. 3). The disorder (*HW*) is also larger in branched MVPBd.

IMMISCIBLE BLENDS

The interchain spacing and half-widths for several amorphous polymer blends are summarized in Table III. Blends of NR with an emulsion SBR, a solution SBR, and branched MVPBd are immiscible; differential scanning calorimetry (DSC) shows two T_gs, and transmission electron micrographs (TEM) indicate the presence of two phases. The experimental data show that the average interchain spacing for an immiscible blend is the weighted average of the interchain spacing of the component homopolymers. The half-width of the blend is also the weighted average of the half-widths of the component homopolymers. This holds true for all immiscible blends listed in Table III. Figure 4 illustrates how closely the experimental data for $\langle R \rangle$ and *HW* for 30/70, 50/50, and 70/30 emulsion SBR/LVPBd blends correspond to the predicted weighted average of $\langle R \rangle$ and *HW* determined from the component polymers. The DSC scans for the emulsion SBR/LVPBd blends all show two T_gs (Fig. 5(a) shows the two T_gs for the 50/50 emulsion SBR/LVPBd blend).

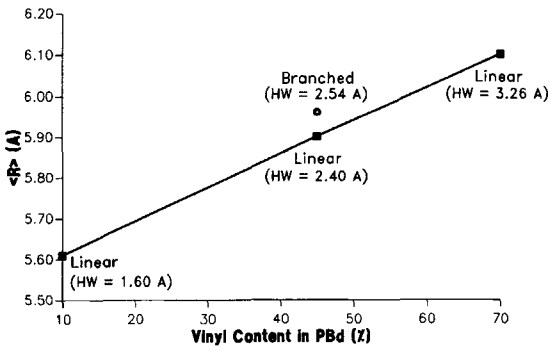

Figure 3 Interchain Spacing for Amorphous PBds.

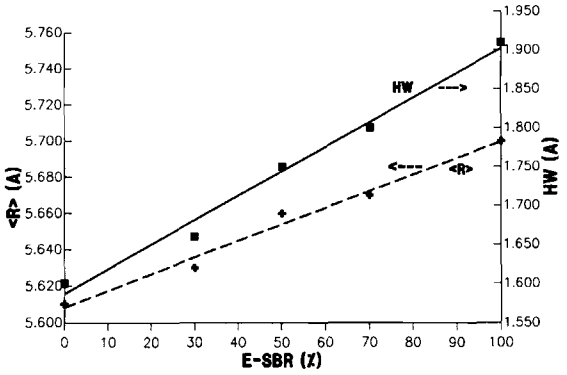

Figure 4 Interchain Spacing and Half-Width for Immiscible Blend: E-SBR/LVPBd.

Inoue et al.[3] showed that X-ray diffraction profiles of polyvinylchloride/polyacrylonitrile butadiene copolymer were the addition of the profiles of the component polymers and that these are two-phase blends. Riga[4] also predicted the wide-angle X-ray result for immiscible blends from their corresponding homopolymers. Our data are consistent with these references. The observed X-ray result for immiscible blends is simply the summation of two separate responses to the X-ray experiment by two physically segregated (with respect to the wavelength of radiation) phases.

MISCIBLE BLENDS

A 50/50 natural rubber (cis-PI) and linear HVPBd (70% vinyl) blend was shown to be miscible as indicated by TEM (one phase) and DSC [single T_g,

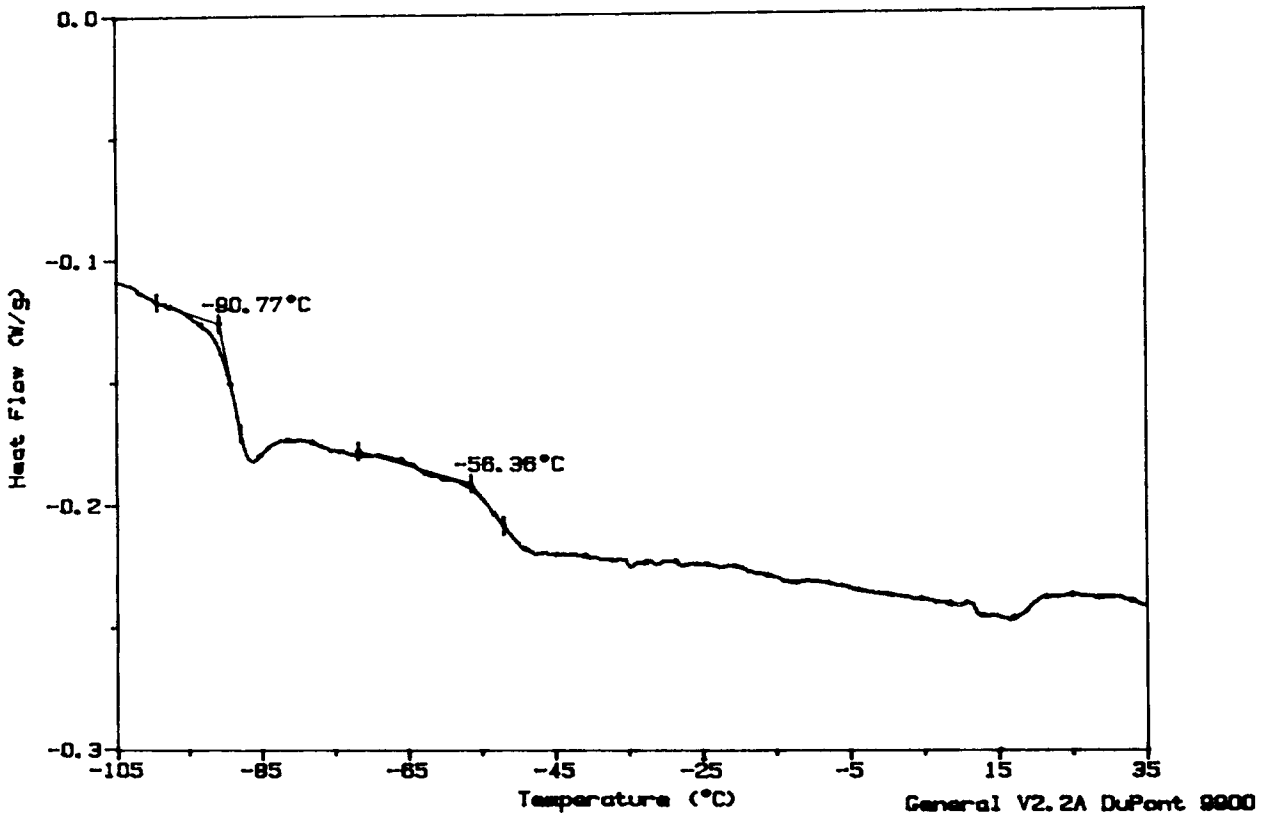

Figure 5(a) DSC for Immiscible Blend: 50/50 E-SBR (23% St)/LVPBd (10% vinyl).

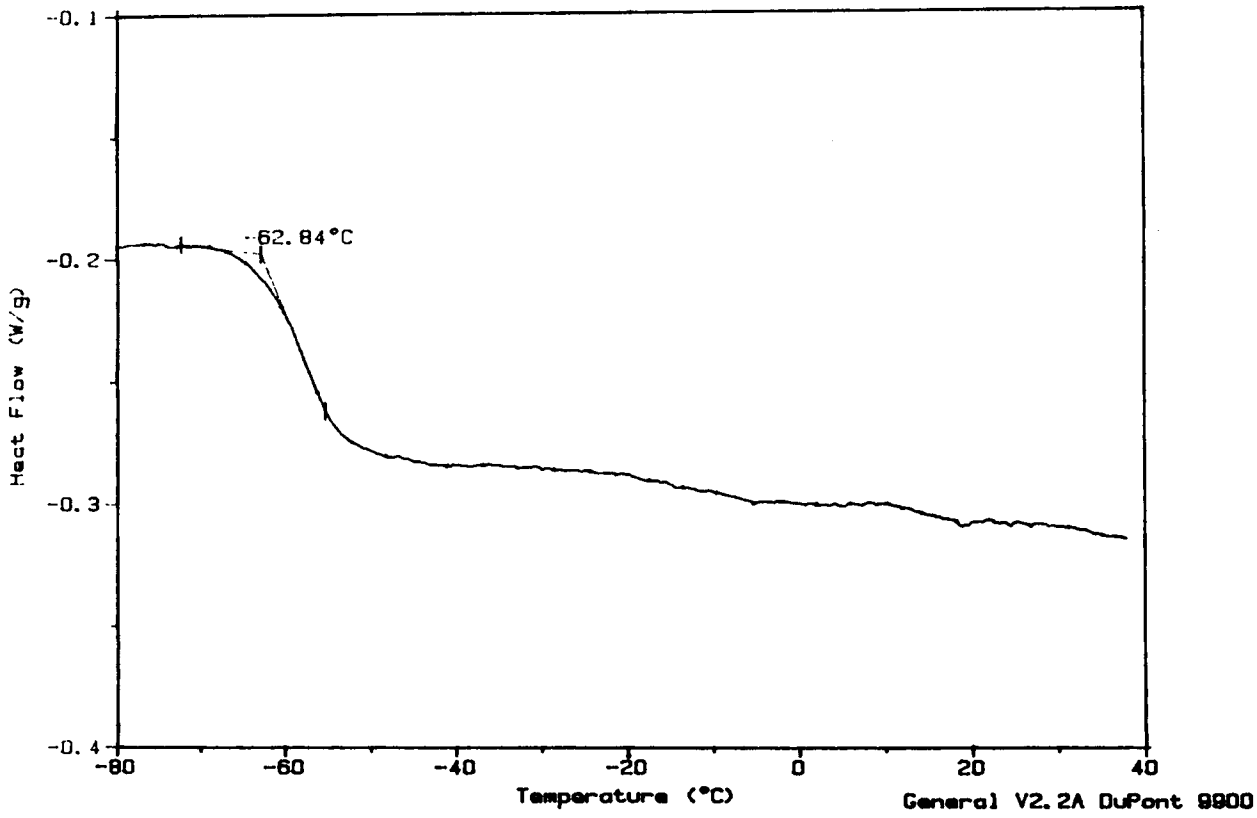

Figure 5(b) DSC for Miscible Blend: 50/50 NR/HVPBd (70% vinyl).

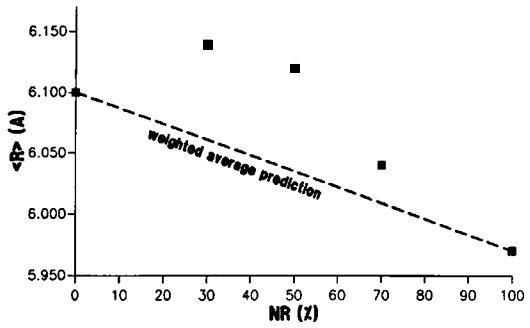

Figure 6 Interchain Spacing for Miscible Blend: NR/HVPBd (70% vinyl).

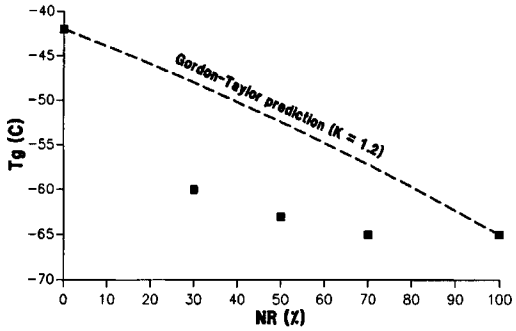

Figure 7 T_g for Miscible Blend: NR/HVPBd (70% vinyl).

Fig. 5(b)]. Earlier results by Cohen also show that HVPBd and cis-PI are miscible.[5] This blend system was investigated by WAXS. Figure 6 shows the experimental $\langle R \rangle$ for blends of natural rubber and HVPBd. The plot for the calculated interchain spacing ($\langle R \rangle$) determined from the weighted average of the component homopolymers is also shown in Figure 6. The interchain spacing for the blend is larger than the weighted average, indicating the formation of a new amorphous structure. The $\langle R \rangle$ values for the 30/70 and 50/50 blends are also larger than those for either component. This larger $\langle R \rangle$ indicates the chains are separated by a larger distance, causing an increase in free volume to accommodate the new packing order. The half-width is similar to the weighted average, indicating that the

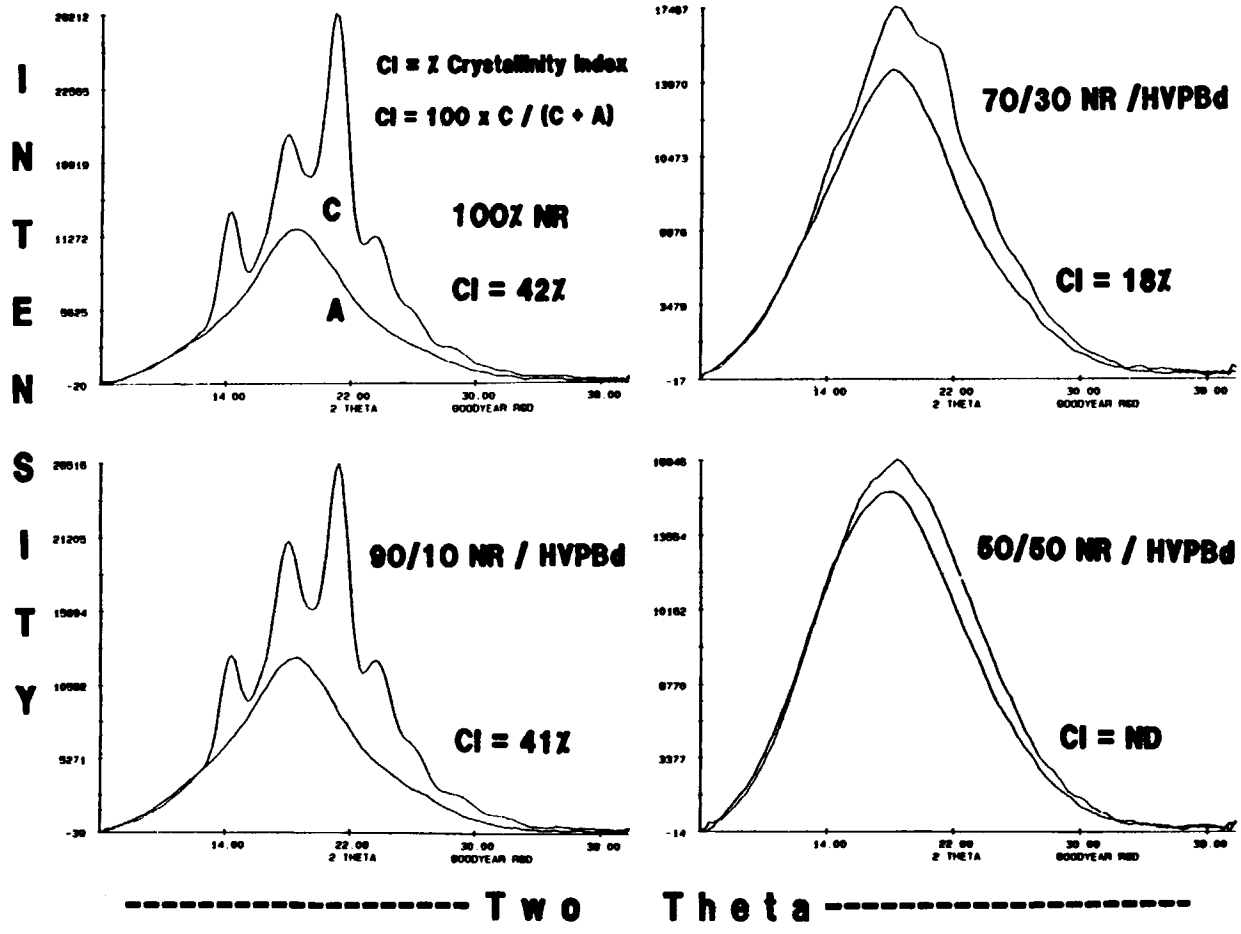

Figure 8 WAXS Profiles for Miscible Blends: NR/HVPBd.

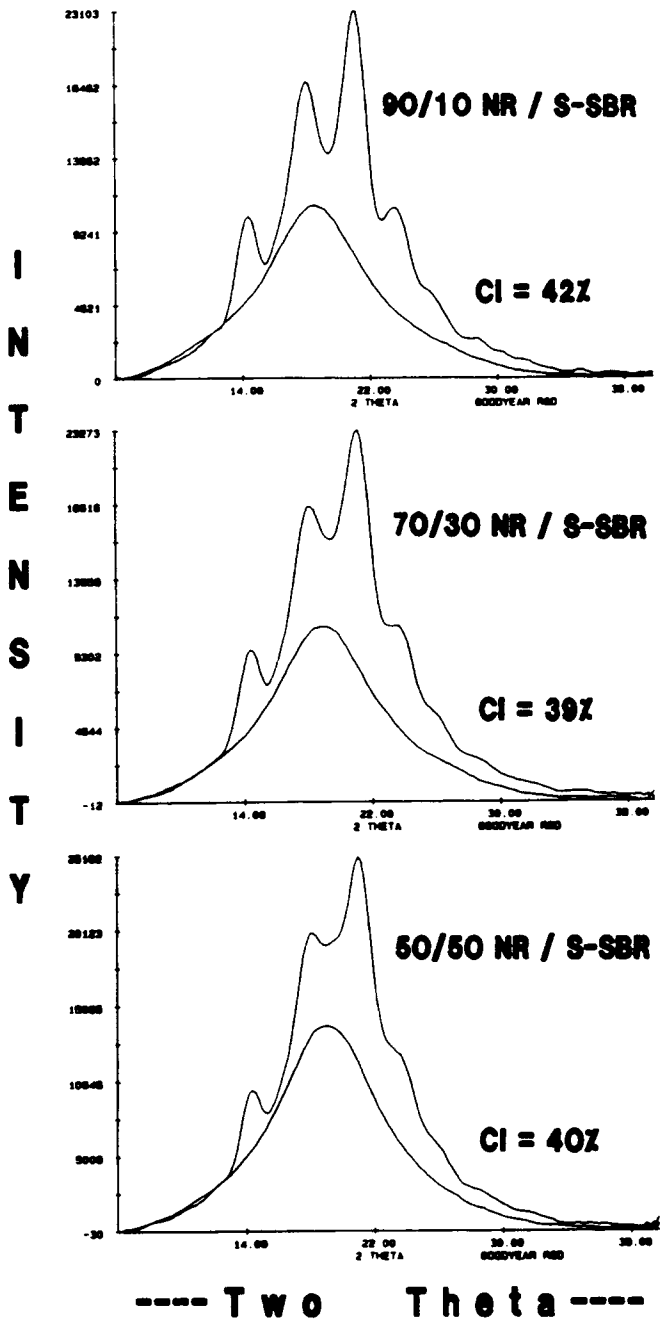

Figure 9 WAXS Profiles for Immiscible Blends: NR/S-SBR (18% St).

new packing order is as efficient. Figure 7 shows the T_gs for the blends and the component homopolymers. The Gordon–Taylor (G–T) equation predicts the T_g for blends based on the blend composition:

$$(T_g - T_{g_A})X_A + K(T_g - T_{g_B})X_B = 0,$$

where $K = \Delta\alpha_B/\Delta\alpha_A$ (where $T_{g_B} > T_{g_A}$), X_A and X_B = weight fractions, T_{g_A} and T_{g_B} = glass transition temperatures, and $\Delta\alpha$ = difference in coefficient of expansion above and below the T_g.

Using $K = 1.2$ ($\Delta\alpha_B = 1.61$ and $\Delta\alpha_A = 1.34$),* the calculated G–T curve predicts much higher T_gs than the observed values (Fig. 7). The lower T_gs for the miscible blends are consistent with an increase in free volume as discussed above.

* Measured by thermomechanical analysis (TMA).

Another illustration of blend miscibility was obtained by calculating the crystallinity of natural rubber in NR/amorphous polymer blends using WAXS profile data. Samples were cooled at −29°C for one to two weeks prior to WAXS measurements. Figure 8 shows the WAXS profiles for the NR/HVPBd blend system. Curve A shows the amorphous blend spectrum obtained at room temperature, while curve C corresponds to the crystalline NR portion (corrected for the amorphous background) of the cooled blend. A crystallinity index (CI) can be calculated as the ratio of the crystalline to the total peak area as shown in Figure 8. Natural rubber alone is 42% crystalline, but its crystallinity decreases as the HVPBd content in the blend increases. For the 50/50 blend, the crystallinity of NR is essentially undetectable. This data suggests that miscibility of HVPBd with NR affected the chain folding of NR and prevented its crystallization. A similar type of behavior is well documented in the literature in which the crystallinity of polyethylene is interrupted by the addition of propylene groups to produce EPR rubber.

Blend immiscibility via WAXS crystallinity measurements is indicated in Figure 9 for a NR/solution SBR (18% styrene) blend system. The crystallinity index for the 50/50 blend is nearly identical to that of NR alone, suggesting two separate phases thus allowing the NR to crystallize. The broader diffraction peaks for the 50/50 blend may be due to smaller crystallites.

The authors thank Professor A. N. Gent (The University of Akron), R. E. Cohen (Massachusetts Institute of Technology), and J. T. Koberstein (University of Connecticut) for their consultation and suggestions. The authors gratefully acknowledge The Goodyear Tire & Rubber Company for allowing this work to be published and for providing the samples.

REFERENCES

1. H. P. Klug and L. E. Alexander, *X-Ray Diffraction Procedures,* John Wiley & Sons, New York, 1974.
2. E. Lauretti and L. Gargani, *Rubber Plast. News,* **17**(17), 18 (1988).
3. T. Inoue and T. Kobayashi, *Poly. Commun.,* **25,** 148 (1984).
4. A. T. Riga, *Poly. Eng. Sci.,* **18,** 1144 (1978).
5. R. E. Cohen and A. R. Ramos, *Adv. Chem. Series,* **176,** 237 (1979).

Received November 20, 1990
Accepted November 27, 1990